Acta Oceanol. Sin., 2017, Vol. 36, No. 7, P. 102–109
DOI: 10.1007/s13131-017-1088-x
http://www.hyxb.org.cn
E-mail: hyxbe@263.net

A spatial resolution effect analysis of remote sensing bathymetry

LIANG Jian[1], ZHANG Jie[1, 2], MA Yi[2]*

[1] Dalian Maritime University, Information Science and Technology College, Dalian 116026, China

[2] The First Institute of Oceanography, State Oceanic Administration, Qingdao 266061, China

Received 3 December 2016; accepted 1 March 2017

Abstract

A spatial resolution effect of remote sensing bathymetry is an important scientific problem. The *in situ* measured water depth data and images of Dongdao Island are used to study the effect of water depth inversion from different spatial resolution remote sensing images. The research experiments are divided into five groups including QuickBird and WorldView-2 remote sensing images with their original spatial resolution (2.4/2.0 m) and four kinds of reducing spatial resolution (4, 8, 16 and 32 m), and the water depth control and checking points are set up to carry out remote sensing water depth inversion. The experiment results indicate that the accuracy of the water depth remote sensing inversion increases first as the spatial resolution decreases from 2.4/2.0 to 4, 8 and 16 m. And then the accuracy decreases along with the decreasing spatial resolution. When the spatial resolution of the image is 16 m, the inversion error is minimum. In this case, when the spatial resolution of the remote sensing image is 16 m, the mean relative errors (MRE) of QuickBird and WorldView-2 bathymetry are 21.2% and 13.1%, compared with the maximum error are decreased by 14.7% and 2.9% respectively; the mean absolute errors (MAE) are 2.0 and 1.4 m, compared with the maximum are decreased by 1.0 and 0.5 m respectively. The results provide an important reference for the selection of remote sensing data in the study and application of the remote sensing bathymetry.

Key words: remote sensing, spatial resolution, water depth remote sensing inversion

Citation: Liang Jian, Zhang Jie, Ma Yi. 2017. A spatial resolution effect analysis of remote sensing bathymetry. Acta Oceanologica Sinica, 36(7): 102–109, doi: 10.1007/s13131-017-1088-x

1 Introduction

Remote sensing bathymetry is a kind of technical method of water depth measurement, which has the advantages of a large area coverage, a speed and an economy. It is especially suitable for the measurement of the coastal shallow water area where the vessel is not accessible. The remote sensing bathymetry should use the remote sensing image data and the water depth control point information, while the remote sensing image usually has the different spatial resolutions, that is, different spatial scales. In the relevant disciplines of spatial information, the issue of scale has always been a hot topic (Woodcock and Strahler, 1987; Lam and Quattrochi, 1992; Atkinson and Kelly, 1997; Marceau and Hay, 1999; Su et al., 2001; Huang and Wu, 2006; Han and Gong, 2008; Ming et al., 2008; Li and Wang, 2013). For remote sensing applications, the spatial scale is an important performance index of the remote sensing image, which represents the ability to distinguish the details of ground features.

Existing research works show that the spatial resolution of the remote sensing image has a very obvious effect on a remote sensing model and method. For the same region remote sensing image with different spatial resolutions, the remote sensing model or method will get different inversion results. These research topics include the selection of the optimal remote sensing scale (Fang et al., 2007; Wang et al., 2007; Ming et al., 2008; Zhou and Zhang, 2011) and the remote sensing scale transformation (Peng et al., 2004; Hu et al., 2011; Luan et al., 2013; Zhang, 2013; Liu, 2014), while the research objects are focused on the remote sensing image classification. It is noticed that Powers et al. (2012) research work shows that the difference in the classification accuracy of wetland remote sensing images with different spatial resolutions can be as large as 12%. Lausch et al. (2013) used 4 and 7 m spatial resolution aerial hyperspectral remote sensing data to carry out a comparative study of forest growth conditions, the results show that the monitoring result of 4 m is better than 7 m. Ma et al. (2014) used six kinds of typical object in the Huanghe Estuary wetland as the object of study, quantitatively analyzed the effects of spatial information compression of the hyperspectral remote sensing image and spatial resolution changes on a ground feature spectral. Similarly for the remote sensing bathymetry inversion, the remote sensing image scale issue cannot be ignored. Different spatial resolution images are not only related to the bathymetry retrieval precision, but also are related to the cost of the remote sensing image, so the image spatial resolution effect of the remote sensing bathymetry is a scientific and engineering issue that deserves attention.

In this paper, QuickBird and WorldView-2 multispectral images which cover the Dongdao Island with a spatial resolution of 2.4 and 2 m respectively are used to conduct the remote sensing bathymetry. Four different spatial resolutions, 4, 8, 16 and 32 m remote sensing images are achieved using a mean filter algorithm simulation. A classic multiband log-linear bathymetry model is applied in water depth remote sensing retrieval experiments, in order to analyze the effect of remote sensing image spatial scales by the inversion accuracies of different resolution im-

Foundation item: The National Key Technology Research and Development Program of China under contract No. 2012BAB16B01.
*Corresponding author, E-mail: mayimail@fio.org.cn

ages, and to find an optimal spatial resolution suitable for the remote sensing bathymetry.

2 Study area and data

The Dongdao Island, the second largest island in the Xisha Islands, is selected as the study area. Its shape is roughly rectangular, northwest to southeast, surrounded by a sand beach. The island lies on a long arc huge reef which is northeast bend. Reef terrain is smooth, and the sea water is clear, so the area is suitable to an optical remote sensing bathymetry inversion.

Two scenes of the remote sensing data are used in this paper. QuickBird multispectral image is obtained on November 11, 2005, and WorldView-2 multispectral image is obtained on September 20, 2012, as shown in Fig. 1 respectively. These images both contain four bands, which are blue, green, red and near infrared. The spatial resolution of QuickBird image is 2.4 m, and the spatial resolution of WorldView-2 image is 2.0 m. Both images are preprocessed by the procedures of a radiance conversion, an atmosphere correction and a space registration.

A remote sensing radiance conversion formula is as follows:

$$L(\lambda_i) = absCalFactor_i \cdot DN_i / \Delta\lambda_i,$$

where $L(\lambda_i)$ is the ith band radiance, and the unit is W/(m²·sr·μm); $absCalFactor_i$ is the ith band absolute calibration coefficient; DN_i is the DN value of the ith band; $\Delta\lambda_i$ is the ith band equivalent bandwidth (effective bandwidth). The ith band absolute calibration coefficient and the ith band equivalent bandwidth can be found in the remote sensing image metadata file.

An atmospheric correction is processed by a professional software. The atmospheric models of the two images are both set to “tropical”, aerosol models are both set to “marine”. After the atmospheric correction, remote sensing reflectance data are obtained.

The positioning accuracy of WorldView-2 image is 2.8 m through the field check points. In this paper, the WorldView-2 image is used as a reference to the QuickBird image, and the registration error is within one pixel.

The ship measurement data originated from the “863” project are used as a depth control and check points in this paper. The *in situ* water depth data were measured by single-beam echo sounding. The water depth thematic map scale is 1:2 000, it is necessary to compare with satellite retrieval depth data. Its amount of depth points is greater than 3×10^4, ranging from 0 to 110 m. Three hundred depth control and check points are selected respectively in a depth range of 0–30 m with 0.1 m interval. The distribution of the control and check points are shown on the left in Fig. 2. In this figure, the red triangles represent the control points, the green dots represent the check points. All points meet the uniformity of the spatial distribution, with the uniform distribution in different water depth scopes. Ten survey lines are also selected from the original ship measurement data, the lines contain 1 768 points in total. The distribution of survey lines is shown in Fig. 2, and each line is numbered 1 to 10 from upper to lower. Colors represent different depths, from red to blue depth increases. It can be seen that the depth changes more intensely on the northeast side of the island than that of the southwest side.

A tide height is queried from tide tables in this paper. QuickBird image forming time is 2005-11-11 T03: 19: 48Z, the corresponding tide height is 0.48 m (National Marine Information Center, 2004); WorldView-2 images imaging time is 2012-09-20 T03: 26: 18Z, corresponding tide height is 0.72 m (National Marine Data and Information Service, 2011).

3 Methods

To simulate different spatial resolution images, a mean filter algorithm is used on the preprocessed QuickBird and WorldView-2 images in this paper to derive 4, 8, 16 and 32 m spatial resolution images. Together with the original image, there are five kinds of spatial resolution. Local details of the original image and the down-scaling resolution images are shown in Fig. 3.

In this paper, we use the same depth points and remote sensing bathymetry inversion model to retrieve the water depth of the different resolution images, and analyze the accuracy of the inversion results. The remote sensing bathymetry inversion model used here is a three band linear-log model (Liang et al., 2015), the formula is as follows:

$$Z = A_0 + A_1X_1 + A_2X_2 + A_3X_3,$$

where $X_i = \ln(R_i - R_{i\infty})$, R_i represents the remote sensing reflectance of each band pixel, and $R_{i\infty}$ is the remote sensing re-

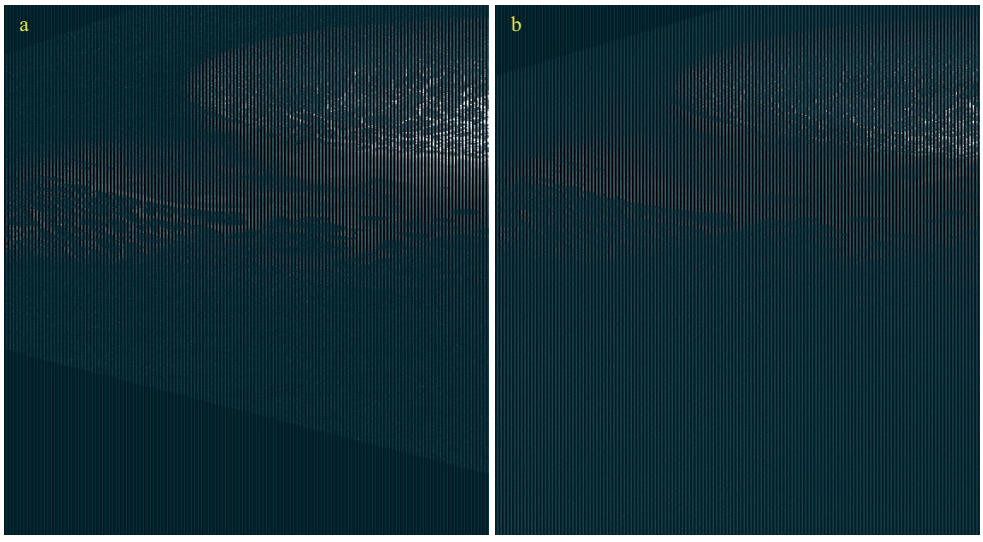

Fig. 1. QuickBird (a) and WorldView-2 (b) multispectral images.

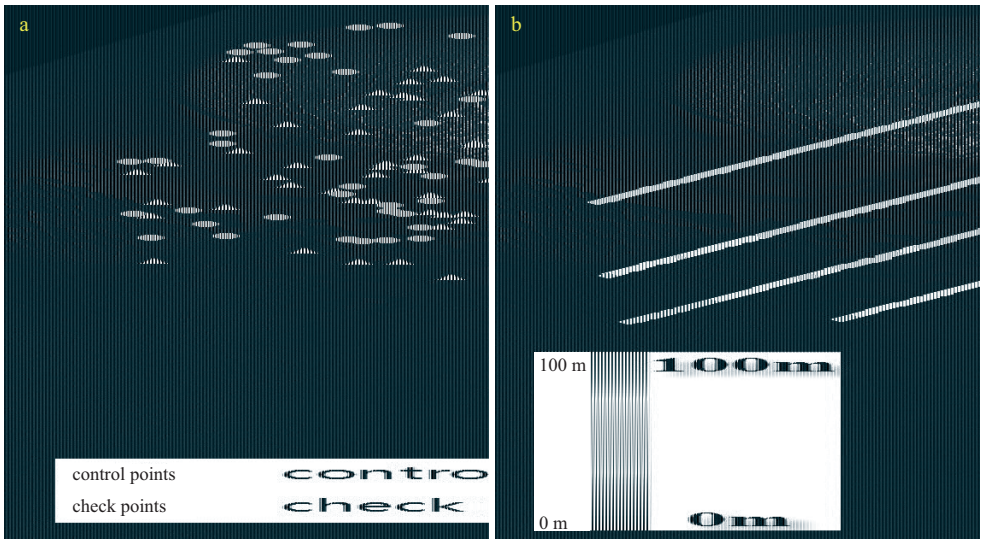

Fig. 2. Distribution of *in situ* water depth points (a) and survey lines (b) of the Dongdao Island.

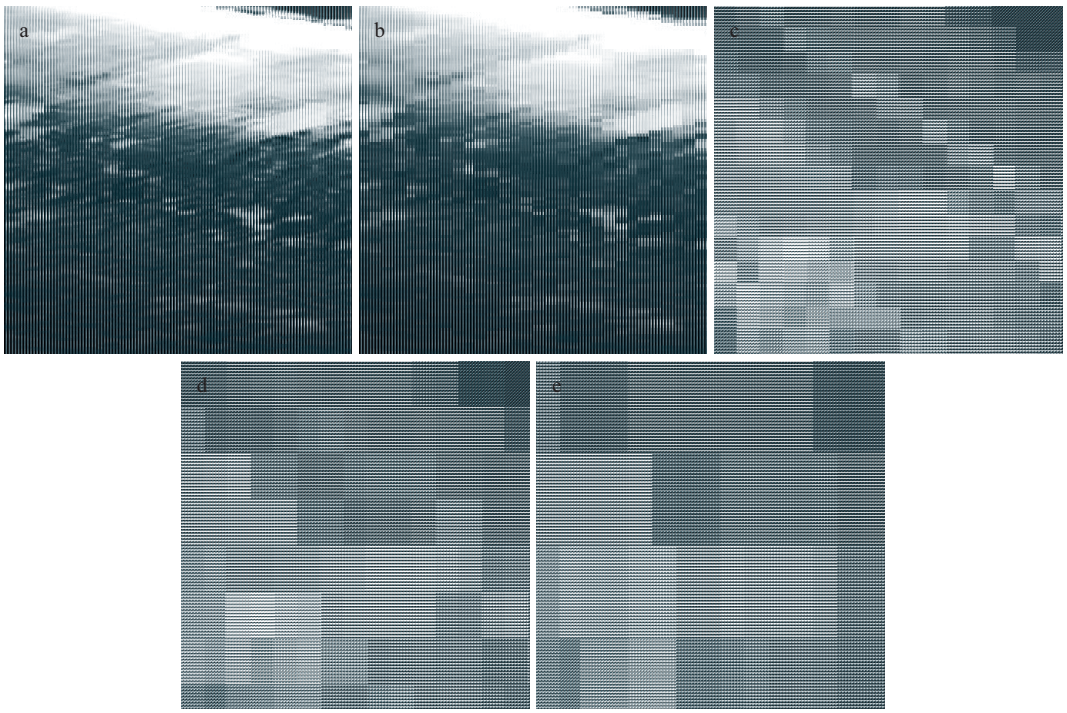

Fig. 3. WorldView-2 multispectral images with different spatial resolution. a. 2 m, b. 4 m, c. 8 m, d. 16 m and e. 32 m.

flectance of the *i*th band in an infinite deep zone; A_0 is a constant; A_1, A_2 and A_3 are the coefficients can be obtained by a regression; and Z represents the depth.

An accuracy is evaluated using the following three indicators: the mean absolute error (MAE), the mean relative error (MRE), and a determination coefficient R^2 which characterize the correlation between the inversion depth and the measured depth.

4 Results and analysis

4.1 *Analysis of overall results*

Figure 4 is the overall evaluation of results of the two images in different resolutions depth inversion. As shown in the figure, with the lower spatial resolution remote sensing images, the MAE and MRE show a phenomenon of decreases first and increases after, the inflection point appeared at the spatial resolution of 16 m. The change of the determination coefficient is slightly different, the QuickBird image bathymetry inversion results of the determination coefficient increase first with image spatial resolution reduction, and reach the top of 0.93 at the spatial resolution of 16 m, then begin to reduce significantly. The determination coefficient of the WorldView-2 image increases with the decrease of spatial resolution, while the spatial resolution is 8 m, the determination coefficient is up to 0.95, then almost unchanges. There is a common denominator in the inversion bathymetry of the two kinds of image that is to meet the MAE, MRE minimum and the determination coefficient maximum conditions, the corresponding image spatial resolutions are both 16 m. It shows that

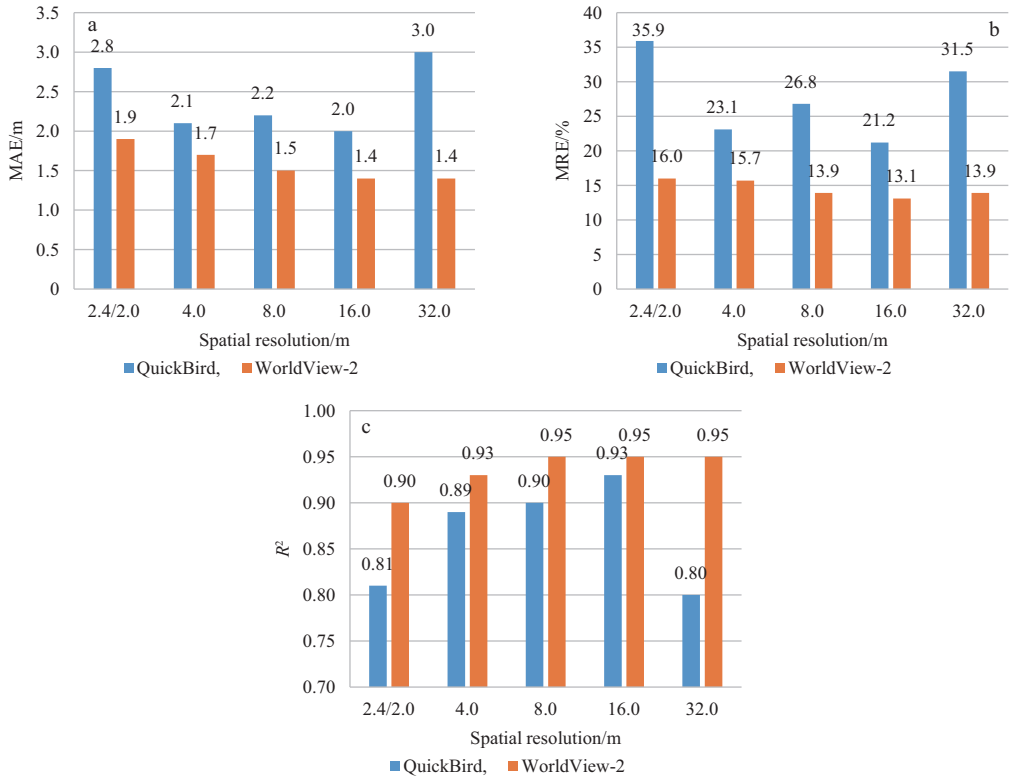

Fig. 4. Evaluation indices of inversion depth from images with different spatial resolution.

the error is minimum and the correlation is the highest when comparing the *in situ* water depth and the remote sensing inversion bathymetry.

Examined from the scatter diagram of inversion bathymetry and check points. The correlation between the true depth values and the inversion values increases first and then decreases with the scale decreases of the remote sensing images. The correlation is the highest when the spatial resolution of the remote sensing image is 16 m. Take Worldview-2 image as an example, the scatter diagram of the inversion depth and *in situ* depth in Fig. 5 from Fig. 5a to d, as the decreasing of spatial resolution, the scattered gradually get closer to the fitting line, while spatial resolution is 16 m this concentration reached the highest level, and then remote sensing image spatial resolution further changes to 32 m, scattered point in Fig. 5e began to appear the trend of dispersion.

4.2 *Analysis of different depth segments*

Analyzed from different water depths, the result then shows a different change trends. In order to better analyze the errors of different water depths on the different scale remote sensing image bathymetry inversions, study regional 0–30 m depth is divided into seven different water depths segment and, the statistics of the spatial resolution of the image, each depth segment of MAE and MRE, the statistical results are shown in Fig. 6 and Tables 1 and 2 respectively.

From the overall change trend, the MAE basically increases with the increase of the water depth, the MRE is just the opposite.

For WorldView-2 image inversion results, in a depth of 0–2 m range, water depth inversion error increases gradually with the scale increase of remote sensing images. The MAE and the MRE are basically consistent with this trend. For the remainder four segments, a situation is contrary to the trend of the water depth in 0–2 m segment, the errors decrease first as the spatial resolution of the remote sensing image scale increases, the minimum error is reach while the image spatial resolution is 16 m, then the errors increase slightly, and the maximum and minimum error value difference is within zero point five times..

As to the inversion results of QuickBird image, the spatial resolutions of the 2.4 m and 32.0 m images in almost all depth of water segments are significantly higher than those in the middle of several sets of the spatial resolution. Spatial resolution 4.0–16.0 m image in the water depth of each has their own advantages and disadvantages, and the difference between each other is not obvious in 0–2, 5–10 and 25–30 m. The depth spatial resolution for 16.0 m image inversion error is minimum; in 2–5, 15–20 and 20–25 m the three depth spatial resolutions for 4.0 m image inversion error are minimum, and the spatial resolution to 8.0 m images in 10–15 m water depth inversion error is minimum.

One of the interpretations for the different spatial resolution remote sensing images in different water depths is the difference between the different water depths and the corresponding region in the space range. For cases on the 0–2 m depth section, the depth space corresponding to the regions is relatively narrow to other area, so that only high spatial resolution remote sensing image can accurately show the detail of depth, for low spatial resolution as it is very easy to smooth out the region, one pixel can cover the water depth from 0 to 2 m, even deeper, leading to lower retrieval accuracy. And for other water depth section area, because the spatial scope is larger, so large scale remote sensing image does not smooth out the corresponding details. Instead, it will have a certain effect of de-noise due to the increase of the scale, so as to improve the accuracy of the inversion. But scale ascension is not without limits, when the remote sensing image scale is sufficiently smooth feature details and the scale lifting will have a negative impact on the water depth inversion. In the

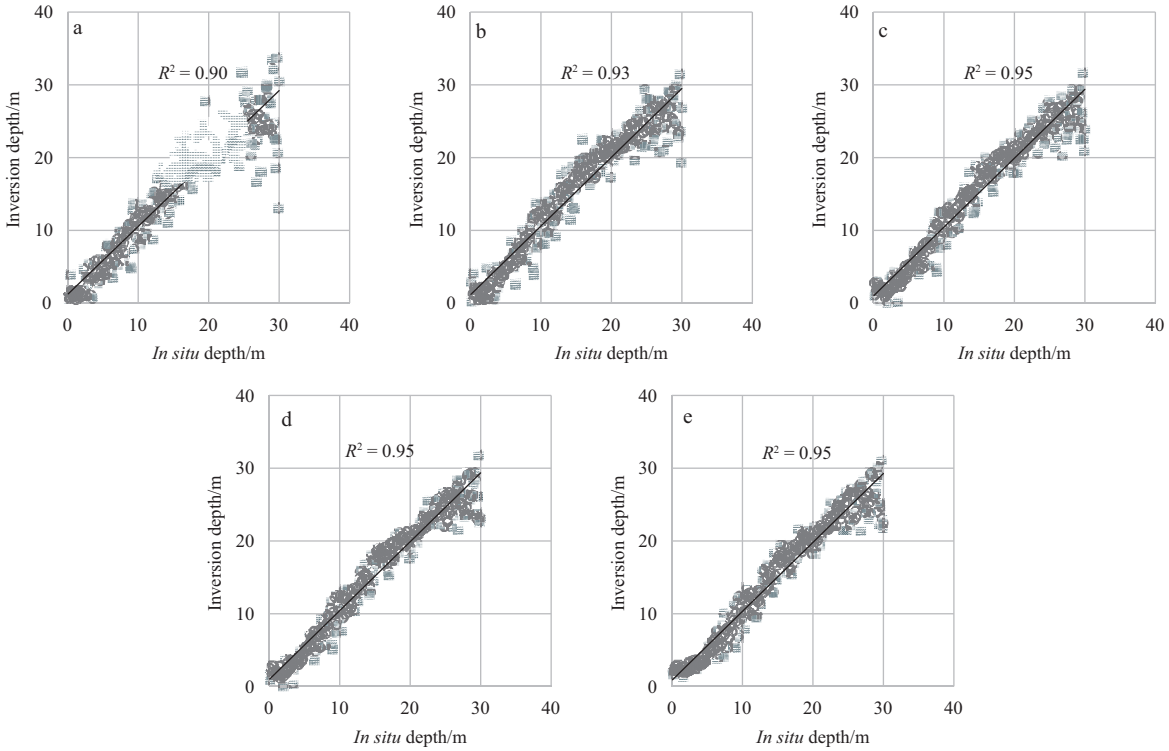

Fig. 5. The scatter plots of the inversion and *in situ* water depths from WorldView-2 images with different spatial resolutions. a. 2 m, b. 4 m, c. 8 m, d. 16 m and e. 32 m.

experimental results of this paper, the spatial resolution of the remote sensing image of 16.0 m can produce the best water depth retrieval results in general.

4.3 *Analysis along survey lines*

In order to further study the influence of the scale change of remote sensing on the detail of water depth retrieval. In this paper, ten water depth lines are extracted, and the measured water depth and the inversion water depth are compared between the ten lines. The results are shown in Fig. 7 (consider all the survey lines are too similar, only Survey lines 1 and 10 are present).

From an overall point of view, when the water depth is shallower than 30 m, the water depth retrieved from different spatial resolution remote sensing images can be consistent with the *in situ* depths; and when the water depth exceeds 30 m, the accuracy will produce swings in water depth inversion. For causes of such a swing, on the one hand is because the water depth control points are located in 30 m to shallower areas, unable to contain 30 m to regional deep water depth; on the other hand the visible light signal in the 30 m to deep area is very weak, noise in corresponding pixel is much larger than the effective signal returning from the bottom, it is difficult to obtain accurate inversion values.

If only focus on regions shallower than 30 m in each section, can also notice to the truth that consistent degree of depth profile of different scale image retrieval and the measured depth profile is not the same. The smaller the spatial resolution is, the difference between the section line of the image and the measured profile is larger than that of the larger scale. In Fig. 7 the swing amplitude of orange line (corresponding to 2/2.4 m image) is larger than that of the green line (corresponding to 32 m image). In order to quantitatively compare the differences between the inversion sections and the measured sections, the mean absolute error and mean relative error have been calculated. As shown in Fig. 8. It can be seen that there are six profile lines (No. 1, 2, 7, 8, 9 and 10) in the ten lines possess the same change characteristics, namely with the increase of remote sensing image scale, the average relative error between water depth inversion value and measured value decreases gradually. This gap is minimal when the image scale is 16 m. When the scale continues to increase to 32 m, the average relative error between the inversion water depth and the measured water depth becomes larger again.

5 Discussion and conclusions

The experimental results from this paper can be found that the spatial resolution of remote sensing images will have different effects on the accuracy of the water depth retrieval. In the spatial resolution of the 2.0/2.4, 4.0, 8.0, 16.0 and 32 m of five kinds of remote sensing images, the overall accuracy of the bathymetry inversion improves as the spatial resolution of remote sensing images decreases, when the spatial resolution is 16 m the accuracy is the highest, followed by a rapid decline. When the spatial resolution is 16 m, the MRE of the water depth of the two scene images is 13.1% and 21.2% respectively, and the maximum error is reduced by 14.7% and 2.9% respectively, the MAE is 2.0 and 1.4 m, compared with the maximum is decreased by 1.0 and 0.5 m respectively. Contrary to the intuitive impression, the original resolution of the image although is the highest spatial resolution, but the bathymetry inversion accuracy is the lowest. Therefore, from the point of view of economy and applicability, it is not necessary to select the image with high spatial resolution in the remote sensing bathymetry inversion. The multispectral images of 16 m can be very compatible to meet the demand.

As used herein, the low spatial resolution images are derived from images of high spatial resolution by using mean filter al-

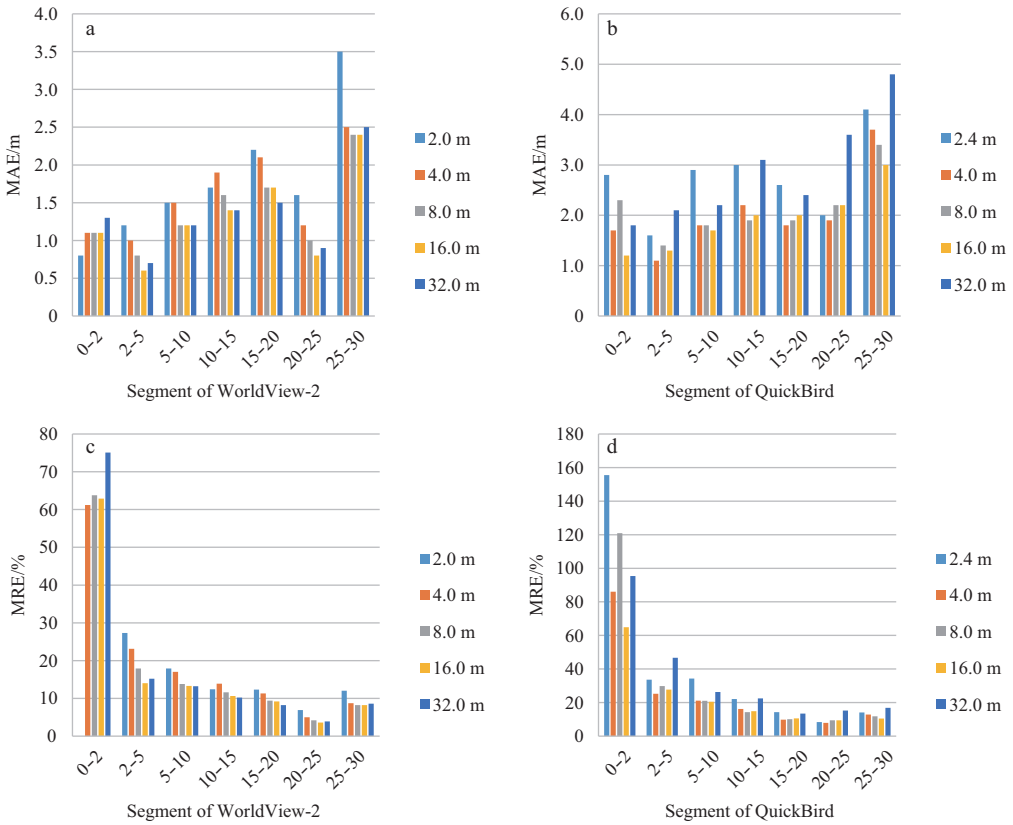

Fig. 6. The MAE and MRE of the inversion depth from images with different spatial resolution.

Table 1. The MAE and MRE of the inversion depth from QuickBird images with different spatial resolutions

No.	Segments	2.4 m		4.0 m		8.0 m		16.0 m		32.0 m	
		MAE	MRE	MAE	MRE	MAE	MRE	MAE	MRE	MAE	MRE
1	0–2	2.8	155.5	1.7	86.0	2.3	120.9	1.2	64.9	1.8	95.4
2	2–5	1.6	33.6	1.1	25.2	1.4	29.8	1.3	27.7	2.1	46.7
3	5–10	2.9	34.3	1.8	21.1	1.8	21.0	1.7	20.5	2.2	26.3
4	10–15	3.0	22.1	2.2	16.2	1.9	14.3	2.0	14.8	3.1	22.5
5	15–20	2.6	14.3	1.8	9.8	1.9	10.1	2.0	10.6	2.4	13.4
6	20–25	2.0	8.4	1.9	7.9	2.2	9.4	2.2	9.4	3.6	15.2
7	25–30	4.1	14.1	3.7	12.8	3.4	11.8	3.0	10.5	4.8	16.8
8	Average	2.8	35.9	2.1	23.1	2.2	26.8	2.0	21.2	3.0	31.5

Table 2. The MAE and MRE of the inversion depth from WorldView-2 images with different spatial resolutions

No.	Segments	2.0 m		4.0 m		8.0 m		16.0 m		32.0 m	
		MAE	MRE	MAE	MRE	MAE	MRE	MAE	MRE	MAE	MRE
1	0–2	0.8	45.4	1.1	61.2	1.1	63.8	1.1	62.9	1.3	75.1
2	2–5	1.2	27.3	1.0	23.1	0.8	17.9	0.6	14.0	0.7	15.2
3	5–10	1.5	17.9	1.5	17.0	1.2	13.8	1.2	13.3	1.2	13.2
4	10–15	1.7	12.4	1.9	13.9	1.6	11.6	1.4	10.6	1.4	10.2
5	15–20	2.2	12.3	2.1	11.3	1.7	9.4	1.7	9.2	1.5	8.2
6	20–25	1.6	6.9	1.2	5.0	1.0	4.2	0.8	3.6	0.9	3.9
7	25–30	3.5	12.0	2.5	8.7	2.4	8.2	2.4	8.2	2.5	8.6
8	Average	1.9	16.0	1.7	15.7	1.5	13.9	1.4	13.1	1.4	13.9

gorithm simulation and resampling. Actual low resolution remote sensing images and the imaging process should be different from the above-mentioned simple simulation. So the best way is to carry out experiments using real different resolution remote sensing image data, but do such way would unavoidably introduced new variables (such as different spectral response, configuration of different wave band, different observation angles, etc.), these all will make the analysis more complex. So the analysis method used in this paper is a compromise, the conclusion still need to validate by large number of practical test.

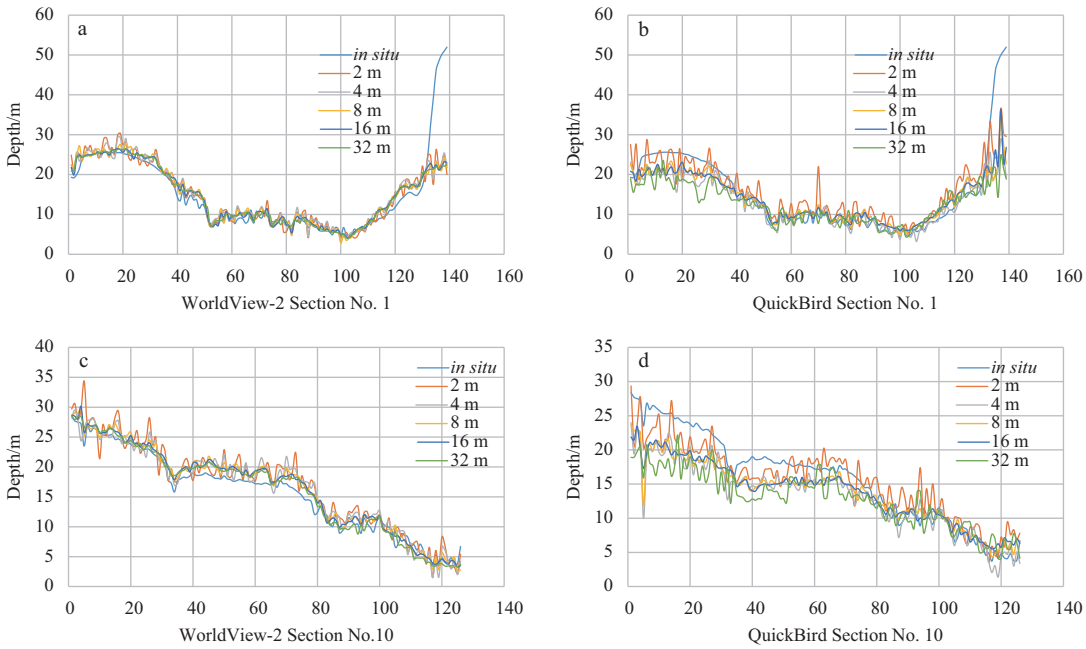

Fig. 7. The inversion depth compared with the measured from sections in images with different spatial resolution.

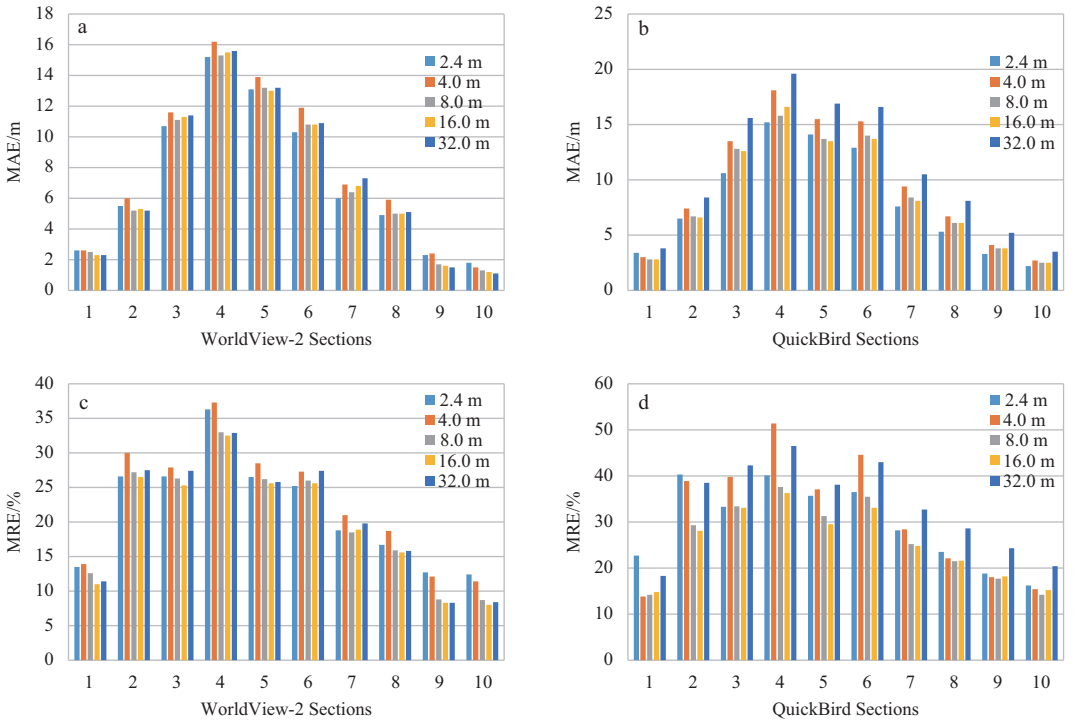

Fig. 8. The MAE and MRE of the inversion depth from sections in images with different spatial resolutions.

References

Atkinson P M, Kelly R E J. 1997. Scaling-up point snow depth data in the U.K. for comparison with SSM/I imagery. International Journal of Remote Sensing, 18(2): 437–443

Fang Bin, Chen Bo, Zhang Yuan. 2007. Research on scale selection and mapping of inspecting biologic diversity using remote sensing. Geography and Geo-Information Science (in Chinese), 23(6): 78–81

Han Peng, Gong Jianya. 2008. A review on cholce of optimal scale in remote sensing. Remote Sensing Information (in Chinese), 23(1): 96–99

Hu Guobiao, Fu Yangbiao, Hu Xiaobao. 2011. Research on remote sensing image scale issue based on variogram suit. Technology Wind (in Chinese), (4): 34–35

Huang Huiping, Wu Bingfang. 2006. Analysis to the relationship of feature size, objects scales, image resolution. Remote Sensing Technology and Application (in Chinese), 21(3): 243–248

Lam N S N, Quattrochi D A. 1992. On the issues of scale, resolution, and fractal analysis in the mapping sciences. Professional Geographer, 44(1): 88–98

Lausch A, Heurich M, Gordalla D, et al. 2013. Forecasting potential

bark beetle outbreaks based on spruce forest vitality using hyperspectral remote-sensing techniques at different scales. Forest Ecology and Management, 308: 76–89

Li Xiaowen, Wang Yiting. 2013. Prospects on future developments of quantitative remote sensing. Acta Geographica Sinica (in Chinese), 68(9): 1163–1169

Liang Jian, Zhang Jie, Ma Yi. 2015. Analysis of the influence of the amount and proportion of control points and check points on the accuracy of bathymetry remote sensing inversion. Marine Science (in Chinese), 39(2): 15–19

Liu Liangyun. 2014. Simulation and correction of spatialscaling effects for leaf area index. Journal of Remote Sensing (in Chinese), 18(6): 1158–1168

Luan Haijun, Tian Qingjiu, Yu Tao, et al. 2013. Review of up-scaling of quantitative remote sensing. Advances in Earth Science (in Chinese), 28(6): 657–664

Ma Yi, Zhang Jie, An Ni. 2014. Spectral fidelity analysis of compressed sensing reconstruction hyperspectral remote sensing image based on wavelet transformation. In: Li Shutao, Liu Chenglin, Wang Yaonan, eds. Pattern Recognition, Berlin Heidelberg: Springer, 138–148

Marceau D J, Hay G J. 1999. Remote sensing contributions to the scale issue. Canadian Journal of Remote Sensing, 25(4): 357–366

Ming Dongping, Wang Qun, Yang Jianyu. 2008. Spatial scale of remote sensing image and selection of optimal spatial resolution. Journal of Remote Sensing (in Chinese), 12(4): 529–537

National Marine Data and Information Service. 2011. 2012 Tide Tables Vol. 3: From the Taiwan Straits to the Beibu Gulf (in Chinese). Beijing: China Ocean Press

National Marine Information Center. 2004. 2005 Tide Tables Vol. 3: From the Taiwan Straits to the Beibu Gulf (in Chinese). Ji'nan: Shandong Cartographic Publishing House

Peng Xiaojuan, Deng Ruru, Liu Xiaoping. 2004. A review of scale transformation in remote sensing. Geography and Geo-Information Science (in Chinese), 20(5): 6–10, 14

Powers R P, Hay G J, Chen G. 2012. How wetland type and area differ through scale: a GEOBIA case study in Alberta's Boreal Plains. Remote Sensing of Environment, 117: 135–145

Su Lihong, Li Xiaowen, Huang Yuxia. 2001. An review on scale in remote sensing. Advance in Earth Science (in Chinese), 16(4): 544–548

Wang Dapeng, Wang Zhoulong, Li Deyi, et al. 2007. Scale of quantitative desertification evaluation by remote sensing. Journal of Natural Disasters (in Chinese), 16(6): 140–144

Woodcock C E, Strahler A H. 1987. The factor of scale in remote sensing. Remote Sensing of Environment, 21(3): 311–332

Zhang Lun. 2013. The information loss of remote sensing image during scaling up procedure (in Chinese) [dissertation]. Beijing: University of Chinese Academy of Sciences

Zhou Mi, Zhang Jielin. 2011. Review on scale transformation for remote sensing image and selection of optimal spatial resolution. World Nuclear Geoscience (in Chinese), 28(2): 94–98